Modeling the hydrogen sulfide binding to heme

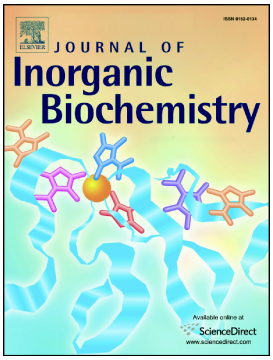

B.D. Ostojić, P. Schwerdtfeger, D.S. Đorđević

PII: S0162-0134(17)30805-X
DOI: doi:10.1016/j.jinorgbio.2018.04.012
Reference: JIB 10479

To appear in: *Journal of Inorganic Biochemistry*

Received date: 18 November 2017
Revised date: 14 April 2018
Accepted date: 17 April 2018

Please cite this article as: B.D. Ostojić, P. Schwerdtfeger, D.S. Đorđević , Modeling the hydrogen sulfide binding to heme. The address for the corresponding author was captured as affiliation for all authors. Please check if appropriate. Jib(2017), doi:10.1016/j.jinorgbio.2018.04.012

Modeling the Hydrogen Sulfide Binding to Heme

B. D. Ostojić[a,*] P. Schwerdtfeger[b] and D. S. Đorđević[a]

[a] *Center of Excellence in Environmental Chemistry and Engineering, Institute for Chemistry, Technology and Metallurgy, University of Belgrade, Njegoševa 12, Belgrade 11000, Serbia*
[b]*Centre for Theoretical Chemistry and Physics (CTCP), The New Zealand Institute for Advanced Study (NZIAS), Massey University Auckland, Private Bag 102904, North Shore City, 0745 Auckland, New Zealand*

Abstract

The binding of hydrogen sulfide to a model heme compound is investigated by coupled-cluster singles-doubles augmented by a perturbative triple excitations, CCSD(T), and density functional theory, DFT. The minimum energy path for the H_2S addition to an isolated heme center of the heme protein is evaluated by adopting as a model the heme compound FeP(Im) (P=porphyrin; Im=imidazole). The FeP(Im)-H_2S aduct is bound by 13.7 kcal/mol at the CCSD(T) level of theory. Relaxed potential energy curves for the lowest lying spin states of the H_2S to FeP(Im) binding using DFT reveal that the binding process is associated with a "double spin-crossover" reaction with the existence of long-distance van der Waals minima only 5-7 kcal/mol above the FeP(Im)-H_2S ground state. The fact that the energy of the singlet ground state of FeP(Im)-H_2S is so close in energy to the dissociation products FeP(Im)+H_2S points towards the reversibility of the H_2S adsorption/desorption process in biochemical reactions.

Keywords: heme; imidazole; H_2S binding; electronic states; density functional theory; coupled cluster theory.

* Corresponding author. E-mail: bostojic@chem.bg.ac.rs (B. D. Ostojić).

Phone: +381 113336893; fax: +381 112636061

1. Introduction

Hydrogen sulfide is present in natural gas, petroleum, volcanic springs and decomposed organic matter. While H_2S is toxic at high concentrations of >600 ppm binding to iron in mitochondrial cytochrome enzymes, at low concentrations it exhibits a variety of important biological functions [1]. The mechanism by which H_2S acts as a signaling molecule in biochemical processes is currently under investigation [2]. Of special interest here is its potential to interact with metal centers in metalloproteins. For example, Vitvicky *et al.* described a new role for hemoglobin (Hb), which in the ferric methemoglobin state binds H_2S and oxidizes it to give a mixture of thiosulfate and iron-bound hydropolysulfides [3]. Boubeta *et al.* found that H_2S is the most favorable species in migration from the bulk to the active site through the internal pathway of a protein [4]. It has been shown that neuroglobin, a kind of a heme enzyme endowed with hexacoordinated iron atoms, can bind H_2S tightly [5]. Ruetz *et al.* have found that human neuroglobin can oxidize H_2S to thiosulfate, albeit inefficiently, but the replacement of the distal histidine ligand by alanine greatly accelerates sulfide oxidation by neuroglobin and supports its oxidation to thiosulfate and to a wide range of catenated sulfur products [6]. As a further example, the nutritional needs of the clam *Lucina pectinata* are in a symbiotic relationship with sulfide oxidizing bacteria. Here, the protein that delivers H_2S to the bacteria is hemoglobin I (HbI), binding H_2S to the ferric heme iron.

Both hemoglobin and myoglobin (Mb) are capable of binding H_2S in the open sixth position of the ferric heme iron [7,8]. It has been proposed that the polarity of the distal heme pocket influences the fate of H_2S bound to the ferric heme [9]. Collman *et al*. revealed that electro-catalytic reduction of oxygen is reversibly inhibited by hydrogen sulfide concentrations similar to those that induce hibernation [10]. It has been proposed that this phenomenon comes from a weak, reversible binding of H_2S to the Fe^{II} porphyrin. Collman *et al*. concluded that at higher concentrations H_2S binds to Fe^{II} in the reduced active site and can act as a competitive inhibitor of enzyme cytochrome c oxidase (Cco), competing with its substrate, O_2, for binding to the reduced $Fe^{II}Cu^{I}$ active site [10]. However, this inhibition should be reversible as O_2 can easily replace H_2S bound to a reduced Fe^{II} site. Bostelaar *et al*. in the study on hydrogen sulfide

oxidation by myoglobin reported that the isotope data does not rule out the presence of the ferrous hydrogensulfide intermediate [11].

Although there are many studies devoted to the interaction of H_2S with heme-containing proteins, there are many unresolved questions related to the interaction of H_2S with the heme metal center and the nature of the H_2S-heme binding, which requires a more elevated quantum theoretical treatment. This is especially the case when regarding the role of different electronic spin states of H_2S binding to Hb, and its influence on the binding energy when solvent effects are included. Since there are data that indicate that H_2S can interact directly with the heme iron center, in this work we aim to analyze the role of different spin states for the H_2S binding to a heme model molecule in detail and evaluate its binding energy by accurate quantum theoretical methods.

2. Computational Details

Molecular models

In order to investigate the binding of H_2S to heme, we studied the reaction Fe^{II}(heme) + H_2S ↔ Fe^{II}(heme)(H_2S) and the corresponding associated electronic states along the reaction coordinate using density functional theory (DFT). The model compound is neutral and includes H_2S bound to the iron center in the sixth coordination position (Figure 1). The heme group is modeled as a porphyrin ring without substituents and with an axially coordinated imidazole (Im) as a model of the proximal histidine, denoted as P(Im). In addition, Coupled cluster calculations were carried out to more accurately determine the Fe^{II}(heme)-H_2S interaction energy for a simplified mimic in which the porphyrin ring was replaced by two bidentate N-donor ligands $C_3N_2H_5^-$ as shown in Figure 1.

DFT calculations

Geometry optimizations without any symmetry constraints for the ground state singlet, triplet, and quintet structures of FeP(Im), FeP(Im)-H_2S and its simplified mimics FeL_2 (NH_3) and FeL_2 (NH_3)-H_2S (where L is $C_3N_2H_5^-$) were performed employing the BP86 functional [12,13]

together with the def2-SV(P) basis set [14]. In addition, relaxed geometries of the singlet, triplet, and quintet electronic states of the H_2S-FeP(Im) system were obtained along the H_2S-Fe reaction coordinate at the BP86/def2-SV(P) level of theory in order to obtain the potential energy curves (PECs) for the H_2S binding process. For this, the Fe-S distance was kept fixed at selected distances while all remaining structural degrees of freedom were relaxed. To include both dispersion and relativistic effects in the energetics, single-point energy calculations for the PECs of the different spin states along the Fe-S bond in FeP(Im)-H_2S complex were performed using the B97-D DFT method [15] and using the second-order Douglas-Kroll-Hess (DKH) relativistic operator together with a larger QZP-DKH basis set [16,17] on top of the BP86/def2-SV(P) optimized structures. This combination of density functionals ensures that both geometries and corresponding bond energies are described reasonably accurate. Additional geometry optimizations employing the B97-D/def2-TZVP and ωBP97X-D/def2-TZVP levels of theory as well as the B97-D functional and def2-TZVP on Fe and def2-SV(P) on C, N, S and H atoms were also performed in order to test the accuracy of our method and basis sets on the optimized structures.

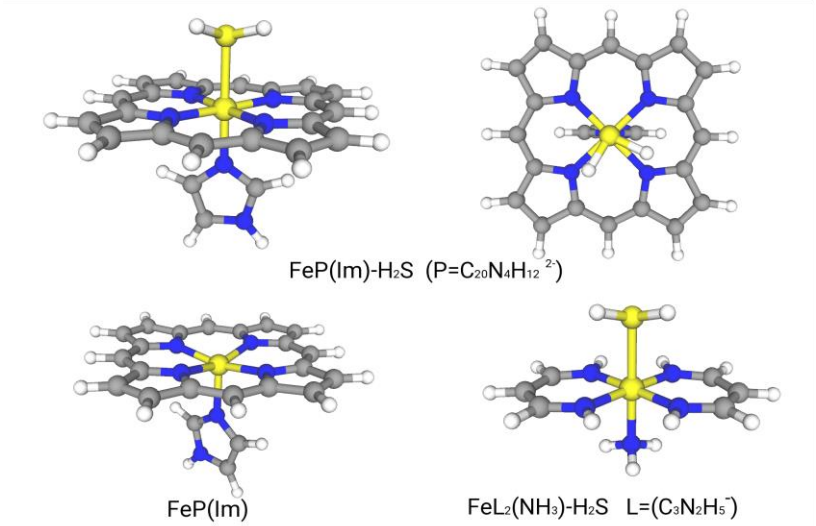

Figure 1. The structural models of the heme and heme-H_2S complexes chosen: FeP(Im) (^{5}A) (bottom left) and FeP(Im)-H_2S (^{1}A) (top right and left), respectively, and the simplified mimic $FeL_2(NH_3)$-H_2S (bottom right) used in the CCSD(T) calculations.

It is well known that some density functional can substantially underestimate or overestimate the binding of molecules to the iron center in porphyrin systems [18]. Therefore, we also explored the accuracy of various DFT approximations to the Fe-S binding energy in the ground electronic state of the FeP(Im)-H_2S complex as well as in the FeL_2(Im)-H_2S mimic at the BP86/def2-SV(P) optimized structures, i.e. several density functionals are employed including: GGA-type functionals, BP86 and B97-D (B97 with Grimme's dispersion correction); the local functional, M06L[19]; hybrid functionals, B3LYP [20], B3LYP* [21,22], TPSSh [23-25] and M06-2X [19]; and the range-separated hybrid functional, ωB97X-D [26]. In particular, we used the ωB97X-D functional for the optimizations of the electronic states of FeP(Im) as it was shown that this functional can correctly predict the ordering of the electronic states of FeP(Im) [27]. Here we note that at the BP86/def2-SV(P) level of theory we are not getting the right ordering of electronic states for FeP(Im), i.e. this functional gives the singlet as lowest energy, while the triplet state and quintet states are 1.63 kcal/mol and 12.33 kcal/mol, respectively, above. Such problems for FeP(Im) were already noted by Radon [28] and Boyd *et al.* [27] who also employed the ωB97X-D functional. For all open-shell electronic states we applied unrestricted Kohn-Sham DFT. The binding energies obtained were corrected for basis set superposition errors (BSSE), scalar relativistic effects using the second-order Douglas-Kroll-Hess Hamiltonian, and zero-point vibrational energy (ZPVE) obtained from the calculated harmonic frequencies. For the relativistic and nonrelativistic binding energies we employed the accompanying cc-pV*n*Z-DK and cc-pV*n*Z basis sets, respectively (*n*=3 for the more important atoms Fe, S and N, and *n*=2 for peripheral atoms C and H). All DFT calculations were carried out with the Gaussian suite of programs [29].

Coupled Cluster Calculations

The application of coupled cluster and related methods for electronic states in bioinorganic systems involving transition metals is given in Refs. [30-33]. For computational efficiency in our single-point coupled cluster calculations we had to employ the small model systems as shown in Fig. 1. The two model systems chosen, $FeL_2(NH_3)$(L=$C_3N_2H_5^-$) and $FeL_2(NH_3)$-H_2S, resemble

the most important features in FeP(Im) and FeP(Im)-H_2S, respectively. The model $FeL_2(NH_3)$ compound differs from the FeP(Im) molecule in conjugation properties, and the whole imidazole ligand is substituted by the simple NH_3 molecule. However, in previous studies on heme-related models it was shown that this mimic can simulate well ligation of the metal center in a porphyrin ring system [28,30,34]. These smaller model compounds have the advantage that they allow for accurate scalar relativistic DKH coupled-cluster singles and doubles augmented by a perturbative triple excitations, CCSD(T), calculations [35-37] in combination with larger sized basis sets. Single point coupled cluster calculations at the CCSD(T) level were carried out with Molpro [38] suite of programs on top of the DFT-optimized structures.

For the iterative coupled cluster term, ΔE_{CCSD}, we include the metal outer-core correlation and obtain the complete basis set (CBS) limit value according to a two-point extrapolation formula introduced by Helgaker *et al.* [39,40], $\Delta E_{int,CBS}(m,n) = (m^3 \Delta E_m - n^3 \Delta E_n)/(m^3 - n^3)$, where m and n are the cardinal numbers of the corresponding correlation consistent basis sets employed. To save computer time, for the non-iterative term accounting for the connected triples in the coupled cluster procedure, $\Delta E_{(T)}$, we took the difference $\Delta E_{CCSD(T)basis5} - \Delta E_{CCSDbasis5}$ with basis 5 chosen as Fe (cc-pwCVTZ-DK); N, S (cc-pVTZ-DK); and H, C (cc-pVDZ-DK). The CCSD T1 diagnostics testing for multireference character gave a value below the suggested threshold of 0.05 [41] for all compounds investigated, while in the case of $FeL_2(NH_3)$-H_2S the D1 diagnostics of 0.17 exceeded the suggested threshold of 0.15 [41] for moderate multi-reference character.

Finally, the coupled cluster binding energies of these model systems were used for an extrapolation procedure introduced by Radon to obtain CCSD(T) estimates for the larger systems [18,28] as discussed in more detail below. Here, different basis sets were used: aug-cc-pwCVTZ-DK, cc-pwCVTZ-DK and cc-pwCVTZ for Fe, cc-pVnZ-DK (n=2,3) and cc-pVnZ (n=2,3) for N and S, and cc-pVDZ-DK and cc-pVDZ for C and H.

3. Results and discussion

Optimized molecular structures

The geometry optimizations of the model system FeP(Im)-H_2S resulted in a $^1A(C_1)$ ground state with a distance between Fe center and the H_2S molecule of $d_{Fe\text{-}S}$ =2.33 Å (see Table 1 for the most important structural data). The H-S bond length in H_2S bound to FeP(Im) is 1.371 Å at the BP86/def2-SV(P) level of theory, and is somewhat longer than the corresponding distance of 1.369 Å for free H_2S (note, at at the B97-D/def2-QZVPPD level of theory we get 1.346 Å in far better agreement with the experimental distance of 1.336 Å [42] or with other more accurate theoretical calculations, see Refs. [43-46]).

It is interesting that the H_2S binding process is accompanied by a substantial structural change in the porphyrin ring system, affecting the orientation of the imidazole plane. In the ground electronic state of FeP(Im)-H_2S, the imidazole plane is in the staggered conformation with respect to the porphyrinato nitrogen atoms (Fig. 1), while in the ground electronic state of FeP(Im) i.e. when H_2S is not bound to Fe, the imidazole plane is in the eclipsed conformation with respect to the porphyrinato nitrogen atoms (Fig. 2). However, we have calculated the barrier to rotation between overlapping and bisecting conformation with respect to the Fe-N_{Pyr} bonds in the ground electronic state of FeP(Im) (^5A) employing the B97-D functional and found a very low value of 1.9 kcal/mol. It is in accordance with other theoretical studies [47,48] that also indicated that this rotation has a very low barrier. On the other hand, the environment of the imidazole ligand in the protein involves a large variety of nearest-neighbour interactions. The nonbonding interactions that come from the protein chain can affect the orientation of the imidazole plane and lead to a hindered rotation. Changing the spin state leads to even more interesting changes in the geometry: while the Fe atom of the FeP(Im)-H_2S aduct in the ^1A ground state lies almost in-plane of the porphyrin ring system (out-of-plane distance is only d_{oop}=0.023 Å), in its quintet ^5A electronic state the Fe atom moves out of the porphyrin plane for both the FeP(Im)-H_2S aduct (d_{oop} =0.246 Å) and FeP(Im) (d_{oop} =0.336 Å), Figure 2. The dihedral angle N_{Pyr}-Fe-N_{Im}-C_{Im} is very small for H_2S-FeP(Im) (^5A) (0.7º) as well as for FeP(Im) (^5A) (0.2º), while in H_2S-FeP(Im) (^1A) the N_{Pyr}-Fe-N_{Im}-C_{Im} angle is about 45º.

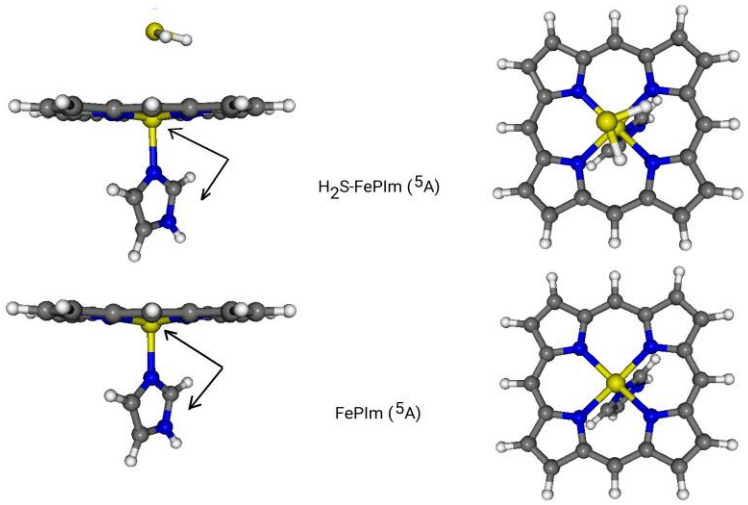

Figure 2. The optimized geometry of FeP(Im) (bottom) and H_2S-FeP(Im) (top) in their quintet electronic states (^{5}A). The arrows indicate main similarities in both structures: the position of Fe below the porphyrin plane and the N_{Pyr}-Fe-N_{Im}-C_{Im} angle is ~0°.

In order to discuss higher spin multiplicities we determined the minimum structures for the possible singlet, triplet and quintet electronic states at the ωB97X-D/def2-SV(P) level of theory. The ground state spin multiplicity of FeP(Im) is quintet in accordance previous theoretical calculations [27,49]. The corresponding triplet and the singlet states are, however, only 1.26 kcal/mol and 7.08 kcal/mol higher in energy, respectively, compared to the quintet ground state. Experimental data on the active sites of myoglobin and hemoglobin protein [50,52] also identified the deoxyheme ground state as a quintet state. The structural parameters of FeP(Im) (^{5}A) that were obtained are consistent with the experimentally obtained high-spin quintet structure of deoxymyoglobin, i.e. see Table 1 where the obtained structural parameters of FeP(Im) are compared with the crystal structure of deoxymyoglobin at 1.15 A resolution by Vojtech *et al.* [53].

The binding energy of H_2S to FeP(Im)

The accurate description of small molecule binding to metalloporphyrins can be a challenging task, especially for DFT in general [18,54,55]. For example, the binding energies for different

spin states in metal containing molecules can vary significantly depending on the density functional chosen [56,63], and a more accurate treatment using multi-reference techniques or coupled cluster procedures is often prohibitive in terms of the computer time involved. However, several well performing density functionals have been recommended for such calculations to correctly determine relative energies between different spin states [25,64-68]. Table 2 contains a summary of the results of our DFT calculations for the H_2S-FeP(Im) and mimic H_2S-$FeL_2(NH_3)$ binding energies corrected for BSSE, scalar relativistic effects and zero-point vibrational energy as described in the computational section.

The data in Table 2 show that the effect of the BSSE on the DFT energetics is only ~1.3 kcal/mol, while relativistic effects are even smaller with ~0.6 kcal/mol. An inspection of the binding energies further reveals that, depending on the functional applied, the differences between calculated binding energies can be significant. Therefore, a better estimate of the Fe-S binding energy in H_2S-FeP(Im) is obtained employing more reliable wavefunction based methods such as coupled cluster theory, CCSD(T), with the aid of the extrapolation procedure introduced in Ref. [28] (more details can be found in Refs. [18,28]). This procedure is based on the observation that DFT results for the spin-state energetics of a full heme model and its simplified L_2-mimic remain in a very good linear correlation [28]. Figure 3 shows the result of this correlation procedure using the data listed in Table 2. We obtain a good linear correlation (correlation coefficient R=0.97, y= 1.12741x + 1.537467) for the H_2S binding energy for both models with seven different DFT methods.

Table 1. Optimized structural parameters for the FeP(Im)-H_2S aduct in the ground and quintet electronic states, and FeP(Im) and mimic in their electronic ground states obtained at the BP86/def2-SV(P) level of theory in comparison with experimental values for deoxymyoglobin.

	Fe-S [Å]	Fe-N_{Pyr} [a] [Å]	Fe-N_{Im} [Å]	Fe-Por plane [Å]	N_{Pyr}–Fe-N_{Pyr} [a] [º]	Fe-S-H [a] [º]	H-S-H [º]	N_{Pyr}-Fe-N_{Im}-C_{Im} [a] [º]	N_{Pyr}-N_{Pyr} [a] [Å]
FeP(Im)-H_2S ^{1}A (min)	2.330 2.339[e]	2.01 2.02[e]	1.959 1.964[e]	0.023 0.004[e]	90.0 90.0[e]	104.5 99.8[e]	91.2 92.5[e]	44.9 44.9[e]	2.84 2.85[e]
FeP(Im)-H_2S ^{5}A	3.4[b] 3.4[e]	2.09[b] 2.08[e]	2.169[b] 2.148[e]	0.246[b] 0.228[e]	89.4[b] 89.5[e]	78.0[b] 58.6[e]	92.1[b] 91.5[e]	0.7[b] 0.5[e]	2.94 2.94[e]
FeP(Im) ^{5}A (min)		2.09 2.08[e] 2.09[d]	2.142 2.139[e] 2.151[d]	0.336 0.274[e] 0.303[d]	88.9 89.3[e] 89.1[d]			0.3 0.0[e] 0.1[d]	2.93 2.93[e] 2.93[d]
FeP(Im) ^{3}A (min)		2.01 2.02[e] 2.02[d]	2.201 2.173[e] 2.219[d]	0.135 0.167[e] 0.116[d]	89.7 89.8[e] 89.8[d]			45.2 44.6[e] 44.7[d]	2.84 2.84[e] 2.84[d]
FeP(Im) ^{1}A (min)		2.00 2.00[e] 2.01[d]	1.884 1.890[e] 1.943[d]	0.143 0.118[e] 0.122[d]	89.7 89.8[e] 89.8[d]			44.9 44.9[e] 44.9[d]	2.82 2.83[e] 2.83[d]
Deoxymyoglobin (exp.)[c]		2.07(3)	2.14(2)	0.390				2.0	2.89(3)
mimic H_2S-$FeL_2(NH_3)$ ^{1}A (min)	2.303 2.298[e]	1.952 1.958[e]	2.029 2.040[e]		89.9 90.0[e]	104.4 103.2[e]	91.9 92.1[e]		2.76 2.77[e]

[a] average of the distances or angles
[b] minimum obtained through the partial optimization with *r*=3.4 Å
[c] X-ray structural data at near-atomic resolution [53]
[d] ωB97X-D/def2-SV(P) optimized structures
[e] optimized structures with B97-D method and the basis sets def-TZVP on Fe and def2-SV(P) on C, N, S, and H

Table 2. Binding energies[a] of H_2S to FeP(Im) and to $FeL_2(NH_3)$ obtained as a single-point energy using different density functionals on top of BP86/def2-SV(P) fully optimized species and including corrections for BSSE, scalar relativistic effects, and zero-point vibrational energies.

	H_2S-FeP(Im)				H_2S-$FeL_2(NH_3)$			
DFT	ΔE_0[b]	ΔE_1[c]	ΔE_2[d]	ΔE_{bind}[e]	ΔE_0[b]	ΔE_1[c]	ΔE_2[d]	ΔE_{bind}[e]
BP86	13.6 (13.8)	12.3 (12.6)	13.0 (13.2)	9.0 (9.2)	12.6	11.4	12.0	8.0
B97-D	16.2 (16.5)	15.0 (15.3)	15.6 (15.9)	11.7 (11.9)	13.0	11.8	12.5	8.4
TPSSh	12.8 (13.1)	11.6 (11.9)	12.3 (12.5)	8.4 (8.5)	11.2	10.1	10.8	6.7
M06L	16.3 (16.6)	15.1 (15.3)	15.6 (15.8)	11.7 (11.8)	13.0	11.9	12.4	8.4
M06-2X	12.1 (12.6)	10.9 (11.3)	11.3 (11.8)	7.4 (7.8)	8.6	7.4	7.9	3.9
B3LYP	6.9 (7.2)	5.6 (5.9)	6.2 (6.5)	2.3 (2.5)	5.6	4.3	4.9	0.9
B3LYP*	6.1 (6.4)	4.7 (4.9)	5.3 (5.5)	1.3 (1.5)	4.9	3.5	4.1	0.1

[a] All values are in kcal/mol. In parentheses are single point energies calculated on top of the fully optimized structures with the B97-D method and the basis sets def2-TZVP on Fe and def2-SV(P) on C, N, S, and H.

[b] Binding energies without BSSE correction

[c] Binding energy corrected only for BSSE

[d] Binding energy corrected for BSSE and scalar relativistic effects

[e] Binding energy corrected for BSSE, scalar relativistic effects and ΔZPVE

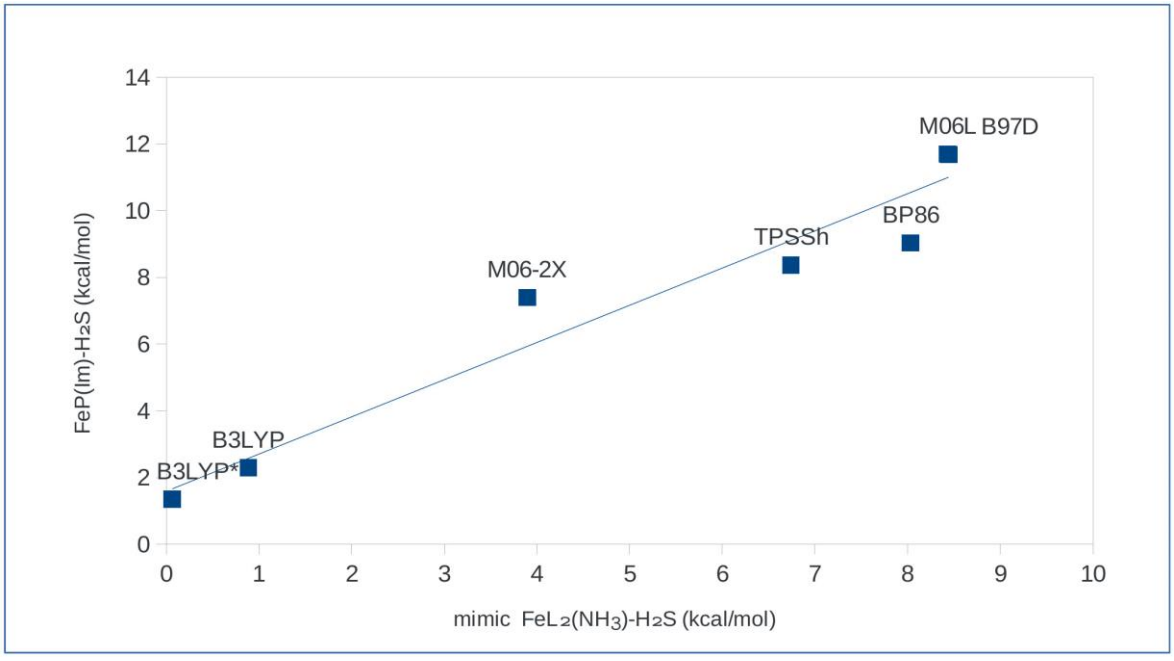

Figure 3. Correlation between the Fe-SH_2 binding energies, BE(Fe-S), for mimic $FeL_2(NH_3)$-H_2S (*x*-axis) and the FeP(Im)-H_2S aduct (*y*-axis) in kcal/mol employing different density functionals including DKH relativistic, BSSE, and ZPVE effects.

The Fe-SH_2 binding energies obtained at the CCSD and CCSD(T) levels for the simplified mimic $FeL_2(NH_3)$-H_2S are summarized for different basis sets and the CBS limit in Table 3. Our final estimate for the binding energy of H_2S to FeP(Im) is 13.7 kcal/mol, obtained on the basis of the fitted line and the CCSD(T) estimate of the binding energy of H_2S to the $FeL_2(NH_3)$ mimic. The best agreement with the CCSD(T) binding energies is achieved for the B97-D and M06L functionals while the worst agreement with CCSD(T) is obtained for the B3LYP and B3LYP* functionals.

The interaction between five-coordinate ferric and/or ferrous heme with bound axial imidazole or 1-methylimidazole (MI) ligand and small gaseous molecules has been the subject of numerous studies. Praneeth *et al.* presented the results of the calculations of the complex formation energy for [Fe(P)(MI)] + NO [69]. The calculations showed that the formation of the nitrosyl complexes is energetically more favorable for ferrous (-11.4 kcal/mol) compared to ferric heme (-3.9 kcal/mol) by ~ 7.5 kcal/mol. The binding of MI to [Fe(P)(X)] (where X=NO, HNO, CO and MI) has been investigated by Goodrich and Lehnart [55]. The calculated ΔG for the reaction of binding MI to FeP(NO) at 298 K is found to be -2.3 kcal/mol overestimating the experimental value by only 0.4 kcal/mol.

It is now interesting to compare our estimated value with the energy difference obtained for the model of the oxyheme complex and deoxyheme + O_2 obtained in theoretical calculations which is 14.9 kcal/mol [70]. Experimental studies indicate that the O_2 addition to hemoglobin and myoglobin is exothermic by 10.3 kcal/mol [71] and 18.1 kcal/mol [72], respectively. Recently, Karpusckin *et al*. reported the first experimental determination of the binding energy of molecular oxygen to a model metal porphyrin complex ion (deprotonated iron(II) tetrakis(4-sulfonatophenyl)porphyrin tetraanion $[Fe^{II}\text{-(tpps)}]^{4-}$) in vacuo [73]. They obtained for the reaction enthalpy (ΔH_r) the value of -9.8 kcal/mol. We applied thermal and entropic corrections calculated using the BP86 method and def2-SV(P) basis set to our estimated binding energy $\Delta E_{estimated}$. Our value for the reaction enthalpy for the association reaction to form the H_2S-FeP(Im) complex is ΔH_r = -10.9 kcal/mol (Table 3). Since the value is comparable to the experimental values for the binding energy between oxyheme complex and deoxyheme + O_2, H_2S can act as an inhibitor competing with O_2 in the binding process to heme, which is one of the reasons for the high toxicity of H_2S.

Table 3. Fe-SH_2 binding energies (in kcal/mol) obtained at the CCSD and CCSD(T) levels of theory for the simplified mimic $FeL_2(NH_3)$-H_2S, derived estimate for the FeP(Im)-H_2S complex based on the correlation plot shown in Fig. 3 and reaction energies for [FeP(Im) + H_2S → FeP(Im)-H_2S] at 298.15 K.

$FeL_2(NH_3)$-H_2S mimic	
[1]ΔE_{CCSD} (basis set 1)	7.66
[2]ΔE_{CCSD} (basis set 2)	3.77
[2]ΔE_{CCSD} (basis set 3)	5.74
[3]$\Delta E_{CCSD}^{CBSlimit}$	6.57
[4]ΔE_{CCSD} (basis set 4)	4.43
[4]ΔE_{CCSD} (basis set 5)	6.40
[5]$\Delta E_{CCSD}^{CBSlimit}$	7.24
[6]$\Delta E_{CCSD(T)}$ (basis set 5)	9.99
[7]$\Delta E_{CCSD(T)}^{CBSlimit}$	10.82
FeP(Im)-H_2S complex	
$\Delta E_{estimated}$	13.74
[8]ΔU_r	-10.30
[8]ΔH_r	-10.94
[8]ΔG_r	3.23

[1] CCSD binding energy corrected for BSSE with DK-relativistic correction; basis set 1: Fe (aug-cc-pwCVTZ-DK); N,S (cc-pVTZ-DK); H,C (cc-pVDZ-DK)
[2] CCSD binding energy corrected for BSSE: basis set 2: Fe (cc-pwCVTZ); N,S (cc-pVDZ); H,C (cc-pVDZ)
basis set 3: Fe (cc-pwCVTZ); N,S (cc-pVTZ); H,C (cc-pVDZ)
[3] CCSD binding energy corrected for BSSE and at the CBS limit (basis sets 2 and 3)
[4] CCSD binding energy corrected for BSSE, with relativistic correction; basis set 4: Fe (cc-pwCVTZ-DK); N,S (cc-pVDZ-DK); H,C (cc-pVDZ-DK); basis set 5: Fe (cc-pwCVTZ-DK); N,S (cc-pVTZ-DK); H,C (cc-pVDZ-DK);
[5] CCSD binding energy corrected for BSSE, with relativistic correction and at the CBS limit (basis sets 4 and 5)
[6] CCSD(T) binding energy corrected for BSSE, with relativistic correction (basis set 5)
[7] CCSD(T) binding energy corrected for BSSE, with relativistic correction and at the CBS limit (basis sets 4 and 5); $\Delta E_{(T)}=\Delta E_{CCSD(T)basis\ 5} - \Delta E_{CCSDbasis\ 5}$
[8] ΔU_r, ΔH_r and ΔG_r values at 298.15 K predicted using $\Delta E_{estimated}$ and thermal and entropic corrections calculated using the BP86 method and def2-SV(P) basis set. $\Delta E_{estimated}$ corresponds to the negative value of the reaction energy.

The minimum energy path for the H_2S binding process

Similar to the O_2 binding to heme [70,74-77], the H_2S addition involves several electronic spin states along the minimum energy path (MEP). As already mentioned, the relative energy between the spin states depends strongly on the DFT approximation applied. To consider important long-range interactions, we calculated the MEP employing the B97-D functional which includes Grimme's dispersion correction (B97-D with relativistic effects included using the QZP-DKH basis sets). The dispersion correction is important in correctly describing the potential energy surfaces and location of crossing points among the different electronic states.

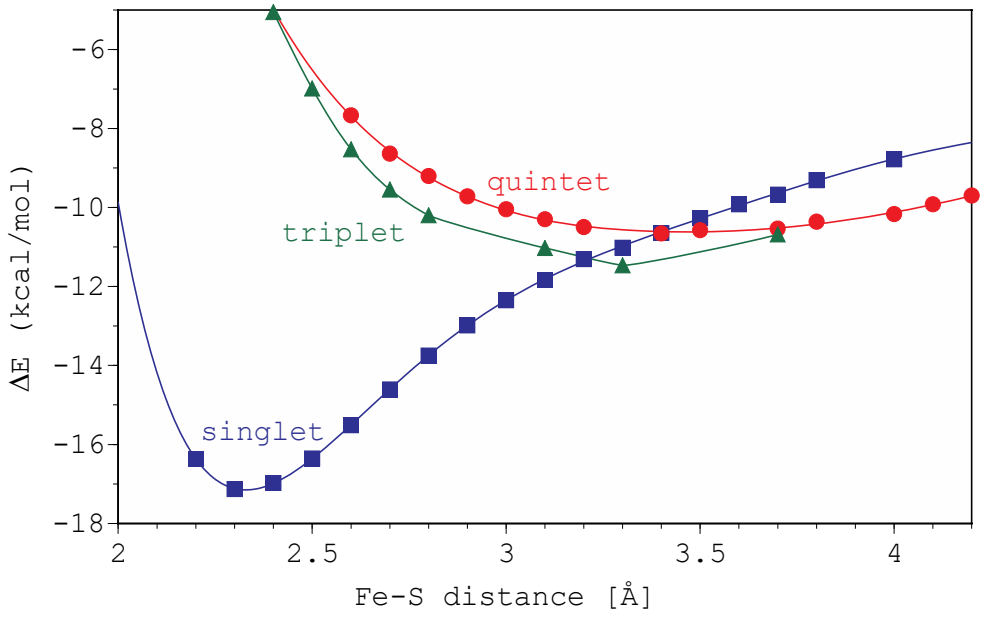

Figure 4. Minimum energy paths for the H_2S binding mode to the FeP(Im) complex calculated at the UB97-D/QZP-DKH//UBP86/def2-SV(P) level of theory relative to the quintet-FeP(Im) + H_2S dissociation limit.

From the potential energy curves we see that the different spin states cross in the formation of the Fe-S bond. This spin-crossing is important as it connects the ground electronic singlet state of FeP(Im)-H_2S with the ground state dissociation products, ^{5}A-FeP(Im) + $^1A_1$-(H_2S), i.e. the dissociation from the ground electronic state of FeP(Im)-H_2S does not occur along the singlet (low-spin) ^{1}A-FeP(Im)-H_2S → ^{1}A-FeP(Im) + $^1A_1$-(H_2S) surface. By moving from the minimum to the lowest dissociation channel (high-spin ground state of ^{5}A-FeP(Im) plus low-spin ground state of singlet H_2S), there are two spin cross-overs: first cross-over point is from the singlet to the triplet state, and the second one is from

triplet to quintet state. Both triplet and quintet electronic states of FeP(Im)-H_2S are characterized by shallow minima, and Fe-S minimum distances longer than that of the singlet state (Figure 4). The potential energy curve of the singlet state has a minimum at 2.3 Å. The quintet and triplet electronic states have long-distance van der Waals minima. The triplet state minimum is placed at ~3.3 Å and ~6 kcal/mol (5.7 kcal/mol) above the ground state minimum, while the quintet state minimum is at ~3.4 Å and ~6 kcal/mol (6.5 kcal/mol) above the ground state minimum. The quintet state crosses the triplet curve at around 3.7 Å, while the triplet state crosses the singlet state at around 3.3 Å. The energy of the singlet-triplet crossing point is about 6 kcal/mol above the ground state minimum. In order to check if the method and the basis set def2-SV(P) used for the geometry optimization are sufficient, we have also performed the constrained geometry optimizations employing the B97-D method and enlarged basis set on Fe (def2-TZVP) and def2-SV(P) on C, N , S and H for the selected geometries (d_{Fe-S}= 2.2, 2.3, 2.5, and 3.5 Å). The single point calculations on top of the obtained structures were done at the same level of theory as the one used for the energies presented in Fig. 4. The energy differences were on average 0.14 kcal/mol (0.181, 0.150, 0.098, and 0.115 kcal/mol) so that it can be concluded that minor differences in the optimized structures are not expected to alter the energetics significantly.

The following observations emerge from the analysis of the potential energy curves in Figure 4. The computed MEPs reveal a crossing region with several low-lying spin states. The triplet and the quintet electronic states are close in energy over a remarkably large fraction of the computed Fe-S distance, and the MEPs for the triplet/quintet crossing are rather shallow. According to Landau-Zener theory [78,79], the crossing probability between two electronic states of different spin multiplicity can be greatly enhanced by the topology of the potential energy surfaces, e.g. small gradient differences between electronic states in the crossing region and a broad crossing region. The addition of H_2S to the FeP(Im) group gives rise first to the formation of a weakly stable van der Waals complex FeP-Im...H_2S, which reaches the quintet-triplet intersystem crossing point and then further to the triplet-singlet intersystem crossing point. The system converts into a singlet state (mainly due to spin-orbit interactions), and a FeP-Im-H_2S complex with the Fe-SH_2 coordination bond is formed. For the FeP(Im)-H_2S→FeP(Im) + H_2S transformation the most stable pathway goes along the singlet state, then after two intersystem crossings (singlet/triplet and triplet/quintet), it reaches the region of the van der Waals minima (5-7 kcal/mol) and dissociates into FeP(Im) plus H_2S. This has a large effect on the binding of hydrogen sulfide to the heme group making the process reversible. It should be noted that the heme molecule possesses the external confinement imposed by the protein environment that can force the Fe-imidazole unit out of the porphyrin ring system and release H_2S molecule with an even smaller activation energy.

In view of the previous studies, such complex behaviour of the potential energy curves was also observed in other heme systems. For example, the major finding of the PES calculations in the study by Preneeth *et al.* is that upon an elongation of the Fe-NO bond of only ~ 0.25 Å the ferric heme nitrosyl passes through at least three different electronic states [69]. Jensen and Ryde concluded that the facile binding of O_2 to hemoglobin and myoglobin arises primarily as an effect of the topology of the binding curves for the relevant spin states caused by the near degeneracy (within 10 kJ/mol) of the triplet and quintet states of deoxyheme [74]. In their study on the FeP(Im)O_2 model they reported a small relative slope of the crossing spin surfaces in the crossing region which ensures large probability for the spin crossing despite modest spin-orbit coupling for iron. They further reported a small energy barrier (less than 15 kJ/mol) having a large effect on the rate acceleration of O_2 binding. This indicates that a similar mechanism applies for the binding of H_2S. Although, the relative energy between spin states depends on the functional applied in the DFT calculations, the results presented in this study permit the basic understanding of the main features of the H_2S addition to heme proteins. Further studies should address how the potential energy surfaces are affected by distal histidine and other protein groups adjacent to the heme center, for example by using QM/MM methods, as well as the diffusion of H_2S towards and from the heme center, and calculate spin cross-over rates from spin-orbit coupling.

5. Conclusions

We have found that the Fe-S bond dissociation in FeP(Im)-H_2S does not proceed on the singlet ground state potential energy surface. Instead, crossings of the different electronic spin states occur to connect the low-spin ground state of FeP(Im)-H_2S with the ground states of the dissociation products ^{5}A-FeP(Im) and $^1A_1$-H_2S. The most stable pathway of the H_2S addition to FeP(Im) starts with the quintet electronic state of FeP(Im). The H_2S binding mechanism has the feature of a "double spin-crossover" reaction as there are two intersystem crossings (quintet/triplet and triplet/singlet) along the Fe-S reaction coordinate. With further shortening of the Fe-S distance, a Fe-S coordination bond is formed with a minimum found at 2.3 Å for the singlet electronic state. The MEPs around the triplet/quintet crossing are rather shallow, leading to a large probability for the spin crossing according to the Landau-Zener formalism. Taking into account that DFT (B97-D) results show the existence of long-distance van der Waals FeP(Im)···H_2S minima that are only 5 - 7 kcal/mol above the ground state minimum, and a small energy difference between H_2S-FeP(Im) complex and FeP(Im) (^{5}A) + H_2S ($^1A_1$) at dissociation - the binding of hydrogen sulfide to the iron of the heme moiety can be considered to be

reversible.

The H_2S to FeP(Im) binding energy has been evaluated from a variety of different DFT methods. We have obtained the final estimate of the binding energy for the H_2S-FeP(Im) complex employing CCSD(T) calculations to be 13.7 kcal/mol. This is comparable to the energy difference between oxyheme and deoxyheme-O_2 complex, and can be of considerable interest due to its relevance for the reversible inhibition of the enzyme citochrome c oxidaze and respiratory chain. We have obtained the reaction enthalpy to be ΔH_r = -10.9 kcal/mol for the association reaction to form the H_2S-FeP(Im) complex, which can be compared to the value of -9.8 kcal/mol for the reaction enthalpy from the recent experimental study on the binding of O_2 to model metal prophyrin complex in vacuo [73].

Abbreviations

BE	binding energy
BSSE	basis set superposition error
CBS	complete basis set limit
CCSD(T)	coupled cluster calculations with singles and doubles augmented by a perturbational correction for connected triple excitations
Cco	Cytochrome c oxidase
DFT	density functional theory
DKH	Douglas-Kroll-Hess relativistic operator
FeP(Im)	P=porphyrin; Im=imidazole
Hb	hemoglobin
Mb	myoglobin
MEP	minimum energy path
PEC	potential energy curves
Pyr	pyrrole subunit
ZPVE	zero-point vibrational energy

Acknowledgments

B.O. and D.Đ. acknowledge financial support from the Ministry of Education, Science and Technological Development (MESTD) of the Republic of Serbia (contract No. ON172001). B.O. and D.Đ. are thankful to the colleagues from the Scientific Computing Laboratory of the Institute of Physics in Belgrade (SCL) for support and help. The molecular simulations were run on the PARADOX cluster at SCL supported in part by MESTD of the Republic of Serbia under project No. ON171017, and on the Massey University CTCP compute cluster supported by the New Zealand Institute for Advanced Study. We are grateful to three anonymous reviewers and editor for their valuable suggestions and helpful comments.

References

[1] O. Kabil, N. Motl, R. Banerjee, Biochim. Biophys. Acta 1844 (2014) 1355–1366.

[2] A.L. King, D.J. Polhemus, S. Bhushan, H. Otsuka, K. Kondo, C.K. Nicholson, J.M. Bradley, K.N. Islam, J.W. Calvert, Y.X. Tao, T.R. Dugas, E.E. Kelley, J.W. Elrod, P.L. Huang, R. Wang, D.J. Lefer, Proc Natl Acad Sci U S A. 111 (2014) 3182–3187.

[3] V. Vitvitsky, P.K. Yadav, A. Kurthen, R. Banerjee, J. Biol. Chem. 290 (2015) 8310 –8320.

[4] F.M.Boubeta, S.E. Bari, D.A. Estrin, L. Boechi, J. Phys. Chem. B 120 (2016) 9642−9653.

[5] T. Brittain, Y. Yosaatmadja, K. Henty, IUBMB Life 60 (2008) 135-138.

[6] M. Ruetz, J. Kumutima, B. E. Lewis, M. R. Filipovic, N. Lehnert, T. L. Stemmler, R. Banerjee, J. Biol. Chem. 292 (2017) 6512-6528.

[7] D.W. Kraus, J.B. Wittenberg, J. Biol. Chem. 265 (1990) 16043-16053.

[8] S. Fernandez-Alberti, D.E. Bacelo, R.C. Binning Jr., J. Echave, M. Chergui, J. Lopez-Garriga, Biophys. J. 91 (2006) 1698–1709.

[9] R. Pietri, A. Lewis, R.G. Leon, G. Casabona, L. Kiger, S.R. Yeh, S. Fernandez-Alberti, M.C. Marden, C.L. Cadilla, J. Lopez-Garriga, Biochemistry 48 (2009) 4881–4894.

[10] J. P. Collman, S. Ghosh, A. Dey, R. A. Decréau, Proc. Natl. Acad. Sci. U. S. A. 106 (2009) 22090−22095.

[11] T. Bostelaar, V. Vitvitsky, J. Kumutima, B.E. Lewis, P.K. Yadav, T.C. Brunold, M. Filipovic, N. Lehnert, T.L. Stemmler, R. Banerjee, J. Am. Chem. Soc. 138 (2016) 8476−8488.

[12] A. D. Becke, Phys. Rev. A 38 (1988) 3098−3100.

[13] J. P. Perdew, Phys. Rev. B 33 (1986) 8822−8824.

[14] F. Weigend, R. Ahlrichs, Phys. Chem. Chem. Phys. 7 (2005) 3297−3305.

[15] S. Grimme, J. Comput. Chem. 27 (2006) 1787−1799.

[16] F. E. Jorge, A. Canal Neto, G. G. Camiletti, S. F. Machado, J. Chem. Phys. 130 (2009) 064108.

[17] G. A. Ceolin, R. C. de Berrêdo, F. E. Jorge, Theor. Chem. Acc. 132 (2013) 1339.

[18] M. Radoń, Inorg. Chem. 54 (2015) 5634−5645.

[19] Y. Zhao, D. G. Truhlar, Theor. Chem. Acc. 120 (2008) 215-241.

[20] A. D. Becke, J. Chem. Phys. 98 (1993) 5648−5652.

[21] M. Reiher, O. Salomon, B. A. Hess, Theor. Chem. Acc. 107 (2001) 48−55.

[22] O. Salomon, M. Reiher, B.A. Hess, J. Chem. Phys. 117 (2002) 4729−4737.

[23] J. M. Tao, J. P. Perdew, V. N. Staroverov, G. E. Scuseria, Phys. Rev. Lett., 91 (2003) 146401.

[24] V. N. Staroverov, G. E. Scuseria, J. Tao, J. P. Perdew, J. Chem. Phys. 119 (2003) 12129.

[25] V. N. Staroverov, G. E. Scuseria, J. Tao, J. P. Perdew, J. Chem. Phys. 121 (2004) 11507.

[26] J.-D. Chai, M. Head-Gordon, J. Chem. Phys. 128 (2008) 084106

[27] V. E. J. Berryman, M. G. Baker, R. J. Boyd, J. Phys. Chem. A 118 (2014) 4565−4574.

[28] M. Radoń, J. Chem. Theory Comput. 10 (2014) 2306−2321.

[29] M.J. Frisch, G.W. Trucks, H.B. Schlegel, G.E. Scuseria, M.A. Robb, J.R. Cheeseman, G. Scalmani, V. Barone, B. Mennucci, G.A. Petersson, H. Nakatsuji, M. Caricato, X. Li, H.P. Hratchian, A.F. Izmaylov, J. Bloino, G. Zheng, J.L. Sonnenberg, M. Hada, M. Ehara, K. Toyota, R. Fukuda, J. Hasegawa, M. Ishida, T. Nakajima, Y. Honda, O. Kitao, H. Nakai, T. Vreven, J.A. Montgomery Jr., J.E. Peralta, F. Ogliaro, M. Bearpark, J.J. Heyd, E. Brothers, K.N. Kudin, V.N. Staroverov, T. Keith, R. Kobayashi, J. Normand, K. Raghavachari, A. Rendell, J.C. Burant, S.S. Iyengar, J. Tomasi, M. Cossi, N. Rega, J.M. Millam, M. Klene, J.E. Knox, J.B. Cross, V. Bakken, C. Adamo, J. Jaramillo, R. Gomperts, R.E. Stratmann, O. Yazyev, A.J. Austin, R. Cammi, C. Pomelli, J.W. Ochterski, R.L. Martin, K. Morokuma, V.G. Zakrzewski, G.A. Voth, P. Salvador, J.J. Dannenberg, S. Dapprich, A.D. Daniels, O. Farkas, J.B. Foresman, J.V. Ortiz, J. Cioslowski, D.J. Fox, Gaussian 09, Revision D.01, Gaussian, Inc., Wallingford CT, 2010.

[30] J. Olah, J. N. Harvey, J. Phys. Chem. A 113 (2009) 7338−7345.

[31] J. N. Harvey, J. Biol.Inorg. Chem. 16 (2011) 831−839.

[32] A. S. Petit, R. C. R. Pennifold, J. N. Harvey, Inorg. Chem. 53 (2014) 6473−6481.

[33] F. Neese, D. Liakos, S. Ye, J. Biol. Inorg. Chem. 16 (2011) 821−829.

[34] A. Ghosh, B.J. Persson, P. R. Taylor, J. Biol. Inorg. Chem. 8 (2003) 507−511.

[35] C. Hampel, K. Peterson, H.-J. Werner, Chem. Phys. Lett. 190 (1992) 1-12.

[36] M. J. O. Deegan, P. J. Knowles, Chem. Phys. Lett. 227 (1994) 321-326.

[37] P. J. Knowles, C. Hampel, H.-J. Werner, J. Chem. Phys. 99 (1993) 5219-5227; Erratum: J. Chem. Phys. 112 (2000) 3106.

[38] MOLPRO is a package of ab initio programs written by H.-J. Werner, P. J. Knowles, G. Knizia, F. R. Manby, M. Schütz, P. Celani, W. Györffy, D. Kats, T. Korona, R. Lindh, A. Mitrushenkov, G. Rauhut, K. R. Shamasundar, T. B. Adler, R. D. Amos, A. Bernhardsson, A. Berning, D. L. Cooper, M. J. O. Deegan, A. J. Dobbyn, F. Eckert, E. Goll, C. Hampel, A. Hesselmann, G. Hetzer, T. Hrenar, G. Jansen, C. Köppl, Y. Liu, A. W. Lloyd, R. A. Mata, A. J. May, S. J. McNicholas, W. Meyer, M. E. Mura, A. Nicklaß, D. P. O'Neill, P. Palmieri, D. Peng, K. Pflüger, R. Pitzer, M. Reiher, T. Shiozaki, H. Stoll, A. J. Stone, R. Tarroni, T. Thorsteinsson, M. Wang .

[39] T. Helgaker, W. Klopper, H. Koch, J. Noga, J. Chem. Phys. 106 (1997) 9639−9646.

[40] A. Halkier, T. Helgaker, P. Jørgensen, W. Klopper, H. Koch, J. Olsen, A. K. Wilson, Chem. Phys. Lett. 286 (1998) 243−252.

[41] W. Jiang, N. J. DeYonker, A. K. Wilson, J. Chem. Theory Comput. 8 (2011) 460−468.

[42] R. L. Cook, F. C. de Lucia, P. Helminger, J. Mol. Struct. 28 (1975) 237-246.

[43] L. Halonen, T. Carrigton, J. Chem. Phys. 88 (1987) 4171.

[44] J. Senekowitsch, S. Carter, A. Zilch, N. C. Handy, P. Rosmus, J. Chem. Phys. 90 (1989) 783.

[45] E. Kauppi, L. Halonen, J. Phys. Chem. 94 (1990) 5779.

[46] I. Kozin, P. Jensen, J. Mol. Spectrosc. 163 (1994) 483.

[47] J.-D. Marechal, G. Barea, F. Maseras, A. Lledos, L.Mouawad, D. Perahia, J. Comput. Chem. 21 (2000) 282.

[48] J.-D. Marechal, F. Maseras, A. Lledos, L.Mouawad, D. Perahia, Chem. Phys. Lett. 353 (2002) 379–382.

[49] H. Nakashima, J. Hasegawa, H. Nakatsuji, J. Comput. Chem. 27 (2006) 426–433.

[50] W. R. Scheidt, C. A. Reed, Chem. Rev. 81 (1981) 543.

[51] L. Pauling, C. D. Coryell, Proc. Natl. Acad. Sci. USA 22 (1936) 210-216.

[52] M. Montenteau, C. A. Reed, Chem. Rev. 94 (1994) 659-698.

[53] J. Vojtechovsky, K. Chu, J. Berendzen, R.M. Sweet, I. Schlichting, Biophys. J. 77 (1999) 2153–2174.

[54] M. Radoń, K. Pierloot, J. Phys. Chem. A 112 (2008) 11824−11832.

[55] L. E. Goodrich, N. Lehnert, J. Inorg. Biochem. 118 (2013) 179−186.

[56] M. Swart, Int. J. Quantum Chem. 113 (2013) 2−7.

[57] M. Costas, J. N. Harvey, Nat. Chem. 5 (2013) 7−9.

[58] P. E. M. Siegbahn, M. R. A. Blomberg, S.-L. Chen, J. Chem. Theory Comput. 6 (2010) 2040–2044.

[59] A. Ghosh, J. Biol. Inorg. Chem. 11 (2006) 712−724.

[60] H. Chen, W. Lai, S. Shaik, J. Phys. Chem. B 115 (2011) 1727−1742.

[61] M. Radoń, E. Broclawik, in Computational Methods to Study the Structure and Dynamics of Biomolecules and Biomolecular Processes - from Bioinformatics to Molecular Quantum Mechanics; Liwo, A., Ed.; Springer: Berlin, 2014; pp 711−782.

[62] J. N. Harvey, DFT Computation of Relative Spin-State Energetics of Transition Metal Compounds. In: Principles and Applications of Density Functional Theory in Inorganic Chemistry I. Structure and Bonding, vol 112. Springer, Berlin, Heidelberg, pp. 151−183.

[63] J. N. Harvey, Annu. Rep. Prog. Chem., Sect. C: Phys. Chem. 102 (2006) 203−226.

[64] M. Swart, A.R. Groenhof, A. W. Ehlers, K. Lammerstsma, J. Phys. Chem. A 108 (2004) 5479−5483.

[65] M. Swart, J. Chem. Theory Comput. 4 (2008) 2057−2066.

[66] S. Ye, F. Neese, Inorg. Chem. 49 (2010) 772−774.

[67] K. P. Jensen, Inorg. Chem. 47 (2008) 10357−10365.

[68] P. E. M. Siegbahn, J. Biol. Inorg. Chem. 11 (2006) 695−701.

[69] V. K. K. Praneeth, F. Paulat, T. C. Berto, S. DeBeer George, C. Näther, C. D. Sulok, N. Lehnert, J. Am. Chem. Soc. 130 (2008) 15288-15303.

[70] J. Ribas-Arino, J. J. Novoa, Chem. Commun. (2007) 3160–3162.

[71] C. R. Johnson, D. W. Ownby, S. J. Gill, K. S. Peters, Biochemistry, 31 (1992) 10074–10082.

[72] M. H. Keyes, M. Falley, R. Lumry, J. Am. Chem. Soc. 1971, 93, 2035-2040.

[73] T. Karpuschkin, M. M. Kappes, O. Hampe, Angew. Chem. Int. Ed. 2013, 52, 1–5.

[74] K. P. Jensen. U. Ryde, J. Biol. Chem. 279 (2004) 14561–14569.

[75] Md. E. Ali, B. Sanyal, P. M. Oppeneer, J. Phys. Chem. B 116 (2012) 5849−5859.

[76] K.K.Kepp, Chem. Phys. Chem. 14 (2013) 3551–3558.

[77] Y. Kitagawa, Y. Chen, N. Nakatani, A. Nakayama, J. Hasegawa, Phys. Chem. Chem. Phys. 18 (2016) 18137-18144.

[78] L. Landau, Physics of the Soviet Union 2 (1932) 46–51.

[79] C. Zener, Proc. R. Soc. London Ser. A 137 (1932) 696–702.

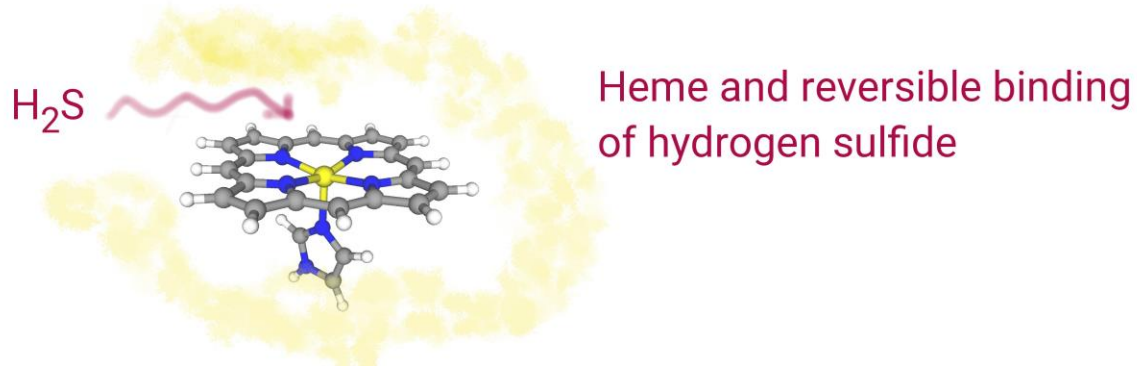

Graphical abstract

Highlights

► The H_2S binding to a heme model molecule is investigated by quantum theoretical methods.
► The binding energy for the H_2S-FeP(imidazole) complex is estimated to be 13.7 kcal/mol.
►Density functional theory (DFT) and coupled cluster calculations (CCSD(T)) are employed.
► Results point towards the reversibility of the H_2S adsorption/desorption process.